JOURNAL OF APPLIED ELECTROCHEMISTRY 24 (1994) 52–57

Effect of ion implantation on the electrochemical behaviour of electrodeposited zinc and chromated zinc layers

M. NIKOLOVA

Institute of Physical Chemistry, Bulgarian Academy of Sciences, Sofia 1040, Bulgaria

K. TAKAHASHI, M. IWAKI

RIKEN (The Institute of Physical and Chemical Research), Hirosawa, Wako-shi, Saitama 351-01, Japan

Received 1 March 1993; revised 5 July 1993

The effect of Ar^+, N_2^+ and O_2^+ implantations on the electrochemical behaviour of electrodeposited zinc with and without chromate coatings has been studied. Cyclic voltammetry in deaerated 0.5 M sodium sulphate solution was used to provide information on the anodic dissolution properties of the specimens. It is shown that N_2^+ implantation on zinc forms an electrochemically inert surface layer. XPS analysis has indicated zinc nitride formation in the N_2^+-implanted layers. Ar^+ and O_2^+ implantations enhance the anodic dissolution of zinc coatings. The higher current may be due to an increase in surface roughness due to the ion beam bombardment, as shown in the electron micrographs. Compact oxide layers could not be formed on zinc by oxygen implantation. It is established that O^+ and N^+ implantations are effective in improving the protective nature of chromate films and oxygen implantation has a stronger effect than the nitrogen implantation. After implantation into chromated zinc layers the reaction current is reduced considerably. It is shown that the implanted specimens maintain low anodic current with repeated potential sweeps. Chromate films become more compact after implantation; this is supported by electron microscopy. Nitrogen is not detected in the N_2^+-implanted chromated zinc electrodeposits. In contrast, Ar^+ implantation causes destruction of the chromate films and the anodic dissolution current is enhanced.

1. Introduction

Electrodeposited zinc layers have been used increasingly as protective-decorative coatings for iron and steel. The sacrificial protective properties of zinc, along with its low price, are the reasons for its wide use in various industries [1]. Much research has been invested to provide brighter zinc deposits with good corrosion protective properties. These properties are improved by formation of conversion chromate films on zinc electrodeposits [2–8]. An increase in corrosion resistance may be achieved by codeposition of small amounts of other metals, as shown in [9–14] and other publications.

Ion implantation has been tested as a modern technique for the formation of corrosion protective surface layers on metals [15–17]. It was shown that ion implantation in steels gave improved corrosion resistance if properly selected implanted elements, fluxes, and energies were used [17]. This technique has the advantage that, unlike coatings, no dimensional changes are made to the structures treated and no discrete interface is produced. The surface modification can be achieved by ion implanting either a passivating element [18–21] or a non-passivating element [22, 23]. The ion implantation of chromium, titanium and lead modifies corrosion behaviour [24]. Chromium implantation inhibits the anodic dissolution of iron [25] and tantalum ions improve the corrosion resistance of iron. The anodic dissolution behaviour of Si and Ti-implanted iron was studied by Okabe *et al.* [26]. The effect of ion implantation was investigated in the case of iron electrodes implanted with nitrogen, argon, zinc, nickel, and chromium [27]. Ashworth *et al.* [28] found that argon implantation in iron resulted in a thickening of the air-formed film. The effect of nitrogen and boron implantation on the corrosion behaviour of iron and stainless steels was investigated by means of a potentiodynamic polarization method [29]. Nitrogen implantation was found to have a positive effect with respect to corrosion inhibition of electrodeposited chromium films [30]. Al-Saffar *et al.* [31] reported that implantation with molybdenum resulted in significant improvement in both the general corrosion and pitting resistance of pure aluminium and a high strength aluminium alloy. Double-ion implantation with both chromium and oxygen was found to be more effective for inhibition of the anodic dissolution of iron than a chromium single-ion implantation [32]. The inhibition of anodic dissolution of the specimens by ion implantation

0021-891X

correlated with the improvement of their corrosion resistance. The technique of double-ion implantation combined with electrochemical oxidation was used for colouring of iron surfaces [33].

In this study ion implantation of Ar^+, N_2^+ and O_2^+ was carried out for the modification of zinc layers electrodeposited on iron from two points of view: (i) to examine the effect of the ion implantation on dissolution of zinc as an electrochemically active metal; and (ii) to reveal the ion implantation effect on the protective nature of chromate layers on zinc.

2. Experimental details

Zinc coatings were deposited on iron specimens from a slightly acidic electrolyte with the following composition (in $g\,dm^{-3}$): $ZnSO_4.7H_2O$ 110; NH_4Cl 30; H_3BO_3 30; and organic additives: polyethylene glycol 8.5; benzylidene acethone 0.6; as per patent composition [34]. The process was performed at a temperature of 20–25° C, pH 4.5 and cathodic current density $2\,A\,dm^{-2}$. The thickness of the zinc coatings was 20 μm. The chromate layers on zinc coated specimens were obtained by treatment of the specimens in solutions for iridescent yellow chromatization [35] at 20–25° C for 30 s. The thickness of the chromate films was approximately 0.5 μm.

Ion implantation of Ar^+, N_2^+ and O_2^+ was carried out with ionic fluxes of $(1.5–2.0) \times 10^{17}$ ions cm^{-2}, at an energy of 150 keV by a 200 kV low current implanter. The pressure of the target chamber and the target temperature during the ion implantation were kept at approximately 1×10^{-4} Pa and 30–80° C, respectively.

Cyclic voltammetry was carried out to provide information on anodic dissolution behaviour of the specimens by using a conventional three-electrode cell system [27]. The zinc coated specimens were used as working electrodes. The potential-sweep rate was $10\,mV\,s^{-1}$. The potential-sweep range was from −1.35 to −1.05 V against a saturated calomel electrode (SCE), which was chosen to measure the anodic dissolution of zinc from preliminary cyclic voltammograms (CVs) within various potential ranges. A 0.5 M Na_2SO_4 solution was used as electrolyte; this was thermostated at 25° C, and deaerated by nitrogen bubbling.

Surface analysis was carried out using X-ray photoelectron spectroscopy (XPS). The surface morphology of the specimens before and after the implantation was studied by scanning electron microscopy (SEM) using a JEOL 53000 unit.

3. Results and discussion

Four of each kind of specimens (nonimplanted, Ar^+-implanted, N_2^+-implanted, O_2^+-implanted electrodeposited zinc, and nonimplanted, Ar^+-implanted, N_2^+-implanted, O_2^+-implanted chromated electrodeposited zinc) were studied. Multisweep cyclic voltammograms (CVs) were measured to compare the effect of ion implantation on the anodic dissolution behaviour of electrodeposited zinc (ZnE) and chromated electrodeposited zinc (Cr–ZnE). Cyclic voltammetry was used as an evaluation method because the implanted layer is gradually changed with dissolution at each potential sweep. The reactivity and durability of the ion-implanted surface layer was evaluated and good reproducibility of the results was achieved.

3.1. *Voltammetric behaviour of the electrodeposited zinc*

The CVs for Ar^+ and O_2^+-implanted ZnE, as shown in Fig. 1(b) and (d), respectively, show higher anodic dissolution currents than that of nonimplanted ZnE (Fig. 1(a)). In contrast, the N_2^+ implantation depresses the anodic current, as shown in Fig. 1(c).

These results suggest that the Ar^+ and O_2^+ implantations enhance the anodic dissolution of zinc; however, the N_2^+ implantation provides an electrochemically-inert surface layer on zinc.

3.2. *Voltammetric behaviour of chromated zinc*

The effect of the ion implantation on the anodic dissolution of Cr–ZnE shows a relatively small current on CVs suggesting that the chromate treatment is effective in protection against the anodic dissolution of zinc. N_2^+ and O_2^+ implantations remarkably depress the reaction currents, which means that ion implantations improve the protective nature of the chromate layers (Fig. 2(c) and (d)). The Ar^+-implanted Cr–ZnE shows higher current (Fig. 2(b)) than those of nonimplanted Cr–ZnE (Fig. 2(a)) and ZnE (Fig. 1(a)).

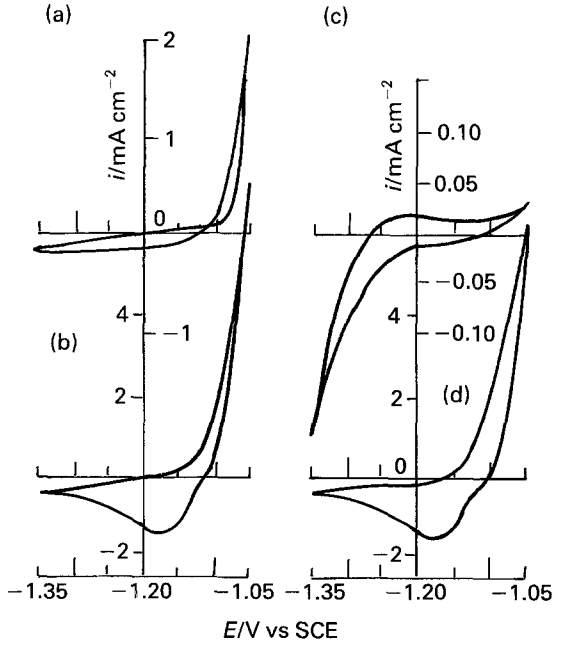

Fig. 1. Cyclic voltammograms at $n_c = 3$ for the ZnE in 0.5 M Na_2SO_4. (a) nonimplanted, (b) Ar^+-implanted, (c) N_2^+-implanted, (d): O_2^+-implanted ZnE.

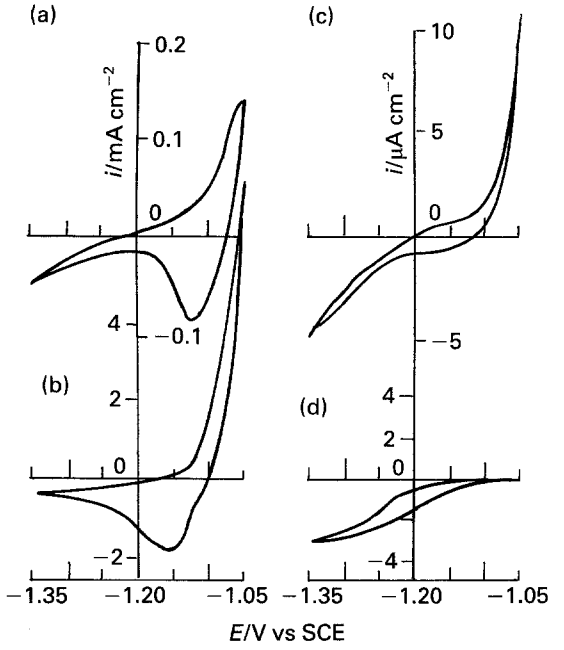

Fig. 2. Cyclic voltammograms at $n_c = 3$ for the Cr–ZnE in 0.5 M Na_2SO_4. (a): nonimplanted, (b): Ar^+-implanted, (c): N_2^+-implanted, (d): O_2^+-implanted Cr–ZnE.

3.3. *Evaluation of dissolution inhibition by the anodic current*

To compare the characteristics of electrodes implanted with various kinds of ions, the anodic dissolution current density at −1.5 V, i_a, at each potential sweep is plotted against the cycle number, n_c. Relatively stable multisweep cyclic voltammograms were obtained within the potential range −1.35 to −1.05 V vs SCE. In the cathodic potential range more negative than −1.35 V hydrogen evolution reaction current increased, so that the potential range for the multisweep cyclic voltammetry is limited up to −1.35 V. When the potential was swept more positive than −1.05 V, the current increased steeply. For this reason the current at $E = -1.05$ V was considered as a value for comparison of the surface layer properties.

Figure 3 shows the i_a–n_c relationship for ZnE. Ar^+ and O_2^+-implanted ZnE, (b) and (d) in Fig. 3, show similar patterns to that of nonimplanted ZnE, (a) in Fig. 3, whereas the currents for implanted ZnE are higher than those for the nonimplanted case. This suggests that implantation of Ar^+ and O_2^+ does not inhibit the anodic dissolution of zinc, and the higher current may be due to the increase in the surface roughness due to the ion bombardment. These results are in good agreement with the results for argon implanted iron [17]. In that case a significant effect of argon implantation on corrosion inhibition cannot be observed because argon implantation results in the formation of radiation damage or bubbles.

The effect of the surface roughness after the ion implantation can be distinctly seen in Fig. 5 for Ar^+-implanted ZnE. The specimen surface exhibits the nonuniformly faceted and cracked surface characteristic of the implanted state. Roughening of

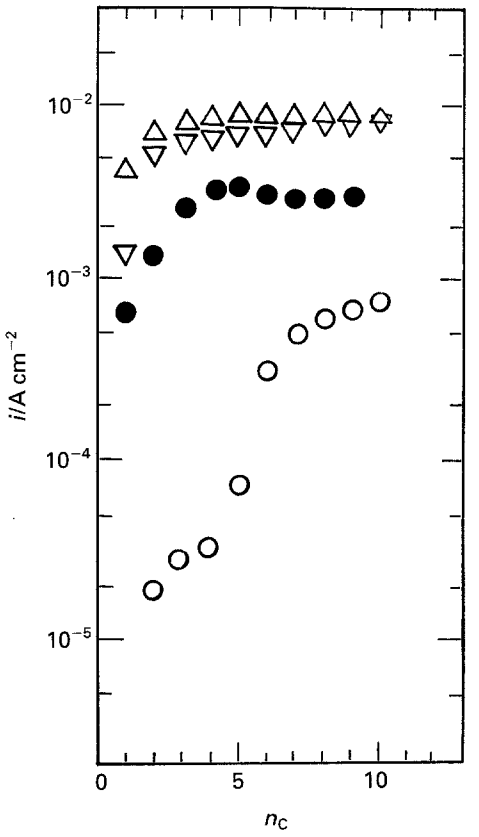

Fig. 3. Anodic dissolution current (i_a) against cycle number (n_c) relationships for the ZnE. (●) Nonimplanted; (△) Ar^+-implanted; (○) N_2^+-implanted; and (▽) O_2^+-implanted. These correspond to (a)–(d) in Fig. 1, resp.

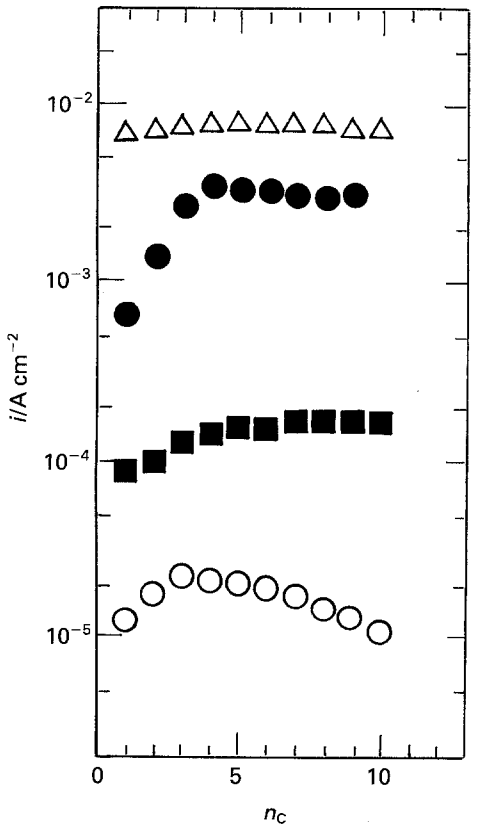

Fig. 4. Anodic dissolution current (i_a) against cycle number (n_c) relationships for the Cr–ZnE. (■) Nonimplanted; (△) Ar^+-implanted; (○) N_2^+-implanted; and O_2^+-implanted Cr–ZnE ($i = 0$). These correspond to (a)–(d) in Fig. 2, resp. (●) Nonimplanted ZnE.

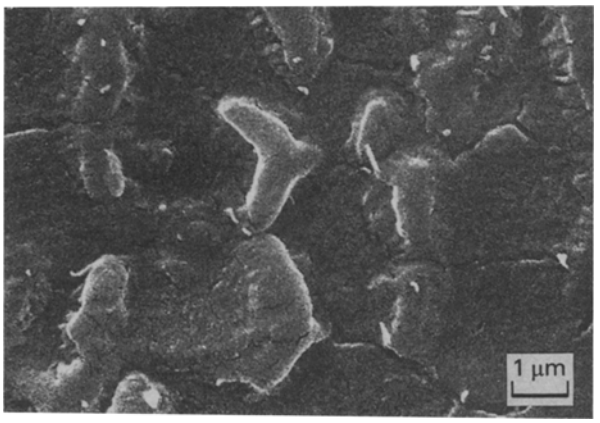

Fig. 5. Electron micrographs of Ar^+-implanted ZnE.

the specimen surface is caused by bubble formation with high dose implantation. The bubble formation may be related to the stability of the elements implanted onto the target material. Argon is unstable in zinc substrate. Zinc oxide is stable as a compound but it does not make a compact oxide layer.

The $i_a - n_c$ relationship for N_2^+-implanted ZnE, (c) in Fig. 3, shows low anodic current at $n_c < 6$, which indicates that the N_2^+-implanted surface layer disturbs the dissolution of zinc. However i_a increases at $n_c > 6$, that is the layer is removed with repeated potential sweeps. XPS analysis has indicated zinc nitride formation in the N_2^+-implanted layer.

Corrosion inhibition by N_2^+ implantation was observed for many specimens, such as pure iron, low carbon steel and tool steel, which had been kept at atmospheric room temperature for a long time. The cavitation (corrosion–erosion) resistance of 1018 steel was improved by nitrogen implantation [36]. It was also considered that the improvement of corrosion inhibition for nitrogen implanted electrodeposited chromium films is due to the fact that implanted nitrogen atoms combine with chromium to form chromium nitrides [30]. These results show that nitride formation may inhibit the corrosion of some metals.

Surface oxide is formed on the freshly N_2^+-implanted ZnE during exposure to the atmosphere; zinc oxide is registered by XPS. The zinc oxide film is not dense but it has been shown [28, 37] that air-formed films tend to grow to a greater thickness on implanted surfaces compared to nonimplanted. This effect may be due to the high defect concentration produced by radiation damage, which stimulates oxidation, and the temperature to which the sample has cooled down to when it is exposed to the atmosphere. The zinc oxide layer is removed by cathodic reduction during cyclic voltammetry.

A significant influence of the ion implantation appeared on the anodic dissolution behaviour of Cr–ZnE, as shown by the $i_a - n_c$ relations in Fig. 4. i_a for the O_2^+-implanted Cr–ZnE, could not be plotted in the Figure, because the i_a's are approximately zero for $n_c = 1-15$.

The figure shows that i_a's of Cr–ZnE (see (a) in Fig. 4) are lower than those of ZnE suggesting that the chromate treatment is effective for corrosion protection of zinc. Further, the currents are significantly

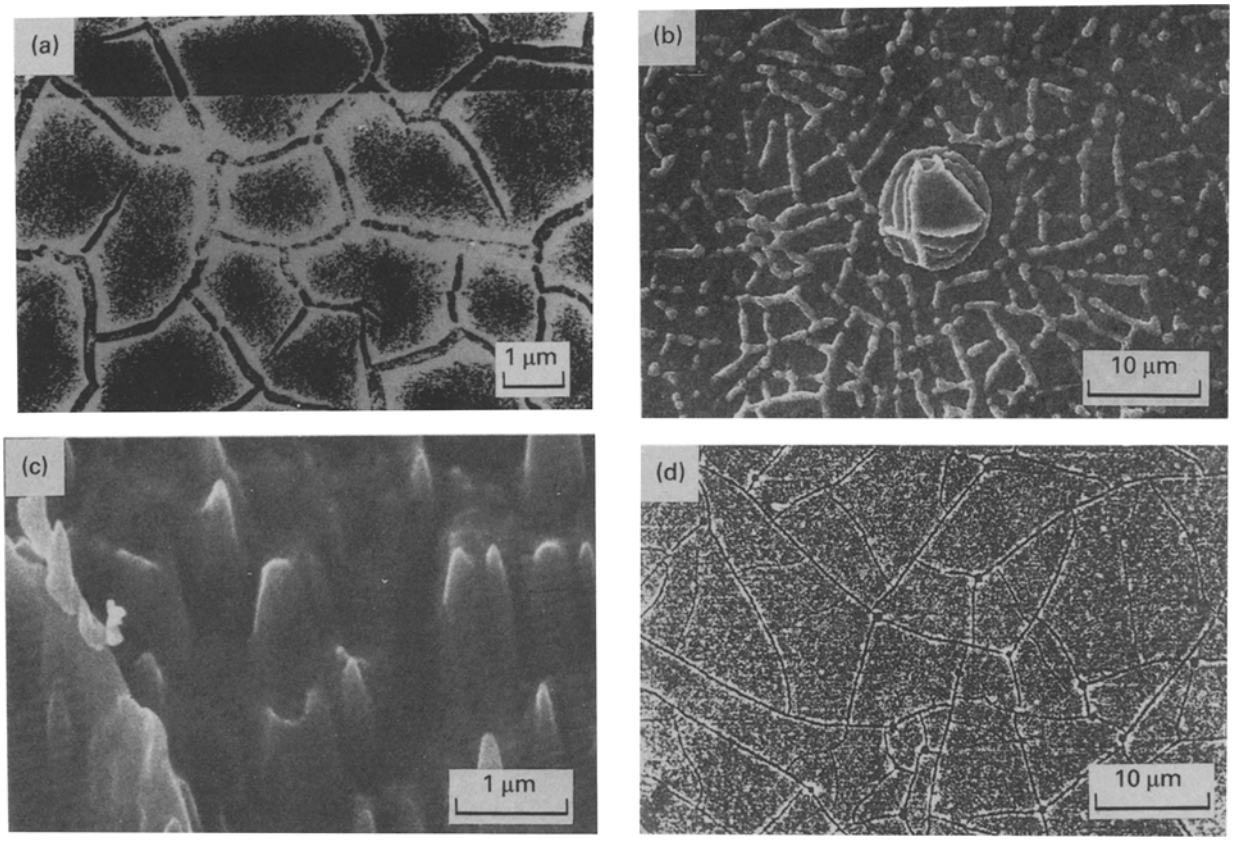

Fig. 6. Electronmicrographs. (a) nonimplanted, (b) Ar^+-implanted, (c) N_2^+-implanted, (d) O_2^+-implanted Cr–ZnE.

lowered by O_2^+ and N_2^+ implantation onto the Cr–ZnE. The O_2^+ and N_2^+-implanted Cr–ZnE maintain low anodic current with repeated potential sweeps. These results show that the ion implantation is effective in improving the protective nature of the chromate layers, due to structural and composition changes of the layers by the ion bombardment. The formation of a compact chromium oxide layer is induced by ion implantation. Figure 6(d) shows the formation of a denser chromate film, as compared with the nonimplanted Cr–ZnE, Fig. 6(a), which demonstrates a close relationship with the decrease in the current density to very small values. In the case of N_2^+ implantation, there are visible changes in the surface structure, Fig. 6(c), as compared with nonimplanted specimens, Fig. 6(a). The chromate films become strong sufficiently to protect the zinc substrate.

The distribution of the elements incorporated into chromate coatings on zinc electrodeposits (Cr–ZnE) was previously investigated by means of Auger analysis [38]. It was shown that chromium is irregularly distributed in the chromate film. Chromium accumulates in the surface layer of the chromate film and its concentration decreases down to the chromate film/zinc interface. In the present work it was established that N_2^+ and O_2^+ implantation onto Cr–ZnE causes chromium to be more regularly distributed across the depth of the chromate films; this is supported by XPS analysis data. Figures 7 and 8 represent the binding energy spectra measured for O_2^+ and N_2^+-implanted Cr–ZnE using XPS combined with argon sputtering. Chromium does not accumulate at the surface layer of the chromate film and the stoichiometry of the chromium oxides does not change through the depth of the film. Nitrogen could not be detected in the N_2^+-implanted

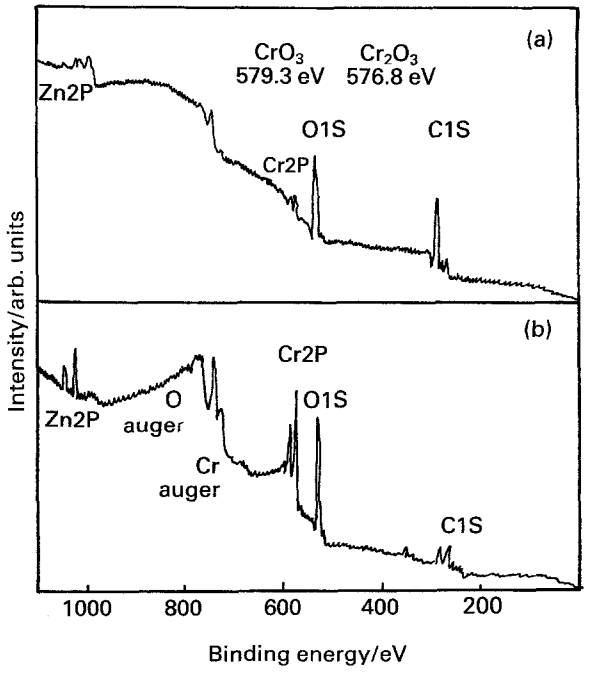

Fig. 7. Binding energy spectra measured by means of XPS. (a) O_2^+-implanted Cr–ZnE; (b) the same specimen after argon sputtering for 30 min.

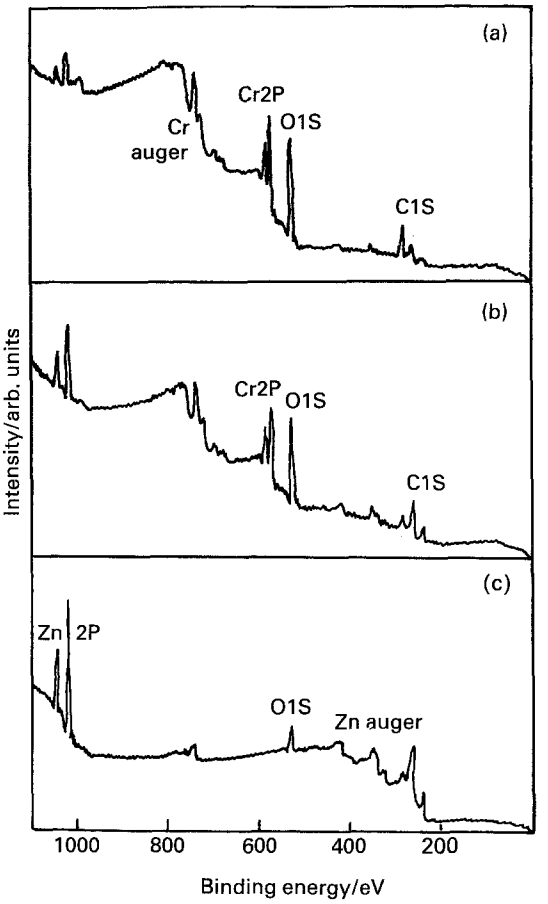

Fig. 8. Binding energy spectra measured by means of XPS. (a) N_2^+-implanted Cr–ZnE; (b) the same specimen after argon sputtering for 30 min; and (c) after argon sputtering for 130 min.

Cr–ZnE specimens. Figure 8(c) shows that after 130 min argon sputtering the chromate film is completely removed from the zinc substrate. It may be concluded that after oxygen and nitrogen implantation, chromate films on zinc become more homogeneous with respect to their composition and structure; this factor improves their protective properties.

On the other hand, Ar^+-implanted Cr–ZnE gives higher i_a's than those of nonimplanted ZnE from the first potential scan; ($n_c = 1$), Fig. 4(b). This is due to visible destruction of the chromate layer on zinc by the Ar^+ implantation, and is supported by electron microscopy, Fig. 6(b). There are holes caused by bubble formation with accumulation of argon in the surface layer. The accumulation may be induced by the low affinity between argon and the chromium oxides. In contrast, the oxygen implanted has a high affinity to the chromium oxides, thus producing a layer of high corrosion resistance.

4. Conclusions

(i) N_2^+ implantation into zinc gives an electrochemically inert surface layer. The anodic current of implanted specimens increases after the six potential sweeps, which indicate that the

layer is removed with repeated cycling. XPS analysis indicated zinc nitride formation in the N_2^+-implanted layers.

(ii) Ion implantations of Ar^+ and O_2^+ are not effective in reducing the anodic dissolution of zinc. The higher anodic current is probably due to increased surface roughness due to the ion beam bombardment. A compact oxide layer could not be formed on zinc by oxygen implantation.

(iii) The anodic dissolution of zinc is inhibited by chromate treatment. The inhibition is considerably improved by O_2^+ and N_2^+ implantation, which produces a highly corrosion resistant surface layer. In this case, implanted specimens maintain low anodic current with repeated potential-sweeps.

(iv) Chromium accumulates in the surface layer of the chromate films on zinc. After oxygen and nitrogen implantation into Cr–ZnE, chromate films become more homogeneous in composition and structure; no accumulation of chromium in the surface layer of the chromate films is registered using XPS and the stoichiometry of the chromium oxides does not change with film depth. Nitrogen could not be detected in the N_2^+-implanted Cr–ZnE by means of XPS analysis.

(v) In contrast, Ar^+ implantation into chromated zinc electrodeposits enhances the anodic dissolution due to destruction of the chromate film on zinc.

References

[1] G. Strube, *Galvanotechnik* **77**(6), (1986) 1318.
[2] E. E. Hall, *Metal Treatment* **14** (1947) 164.
[3] W. E. Pocok, *Met. Finish.* **53**(1), (1955) 80.
[4] R. Biefinger, 'Vem-Handbuch Galvanotechnik, VEB Vorlag Technik, Berlin (1958) p. 181.
[5] F. W. Eppensteiner and M. R. Jenkins, *Met. Finish.* **73**(9), (1975) 29.
[6] F. F. G. Williams, *Plating* **59**(10), (1972) 931.
[7] R. E. Van de Leest, *Werkst. Korros.* **29**(10), (1978) 648.
[8] S. Spring and K. Woods, *Met. Finish.* **79**(6), (1981) 49.
[9] A. Brenner, 'Electrodeposition of Alloys', Vol. 1, Academic Press, New York and London (1963).
[10] T. Amaniya, M. Omura, K. Matsudo and H. Naemura, *Plat. Surf. Finish.* **68**(6), (1981) 96.
[11] V. Roman, M. Pushpavanam, S. Jayakrishnan and B. A. Shenoi, *Met. Finish.* **81**(5), (1983) 85.
[12] G. Ramesh Bapu, G. Devaraj, J. Ayyapparju and R. Subramanian, *ibid.* **85**(2), (1987) 49.
[13] E. Knaak, H. Kohler and I. Hadley, *Metalloberflacke* **39**(4), (1985) 139.
[14] Richard Sard, *Plat. Surf. Finish.* **75**(30), (1987) 30.
[15] M. Naka, K. Hashimoto and T. Masamoto, *Corrosion* **32** (1976) 146.
[16] C. R. Clayton, *Nucl. Instr. & Methods* **182/183** (1981) 865.
[17] M. Iwaki, *CRC Crit. Rev. Solid State & Mater. Sci.* **15**(5), (1989) 475.
[18] V. Ashworth, D. Baxter, W. A. Grant and R. P. M. Procter, *Corros. Sci.* **16** (1976) 755.
[19] V. Ashworth, D. Baxter, W. A. Grant and R. P. M. Procter, *Corr. Sci.* **17** (1977) 947.
[20] B. S. Covino, Jr., P. B. Sartwell and P. B. Needhams, *J. Electrochem. Soc.* **125** (1978) 366.
[21] S. B. Agarwal, Y. F. Wang, C. R. Clayton, H. Herman and J. K. Hirvonen, *Thin Solid Films* **63** (1979) 19.
[22] V. Ashworth, W. A. Grant, R. P. M. Procter and E. J. Wright, *Corr. Sci.* **18** (1978) 681.
[23] Q. M. Chen, H. M. Chen, X. D. Bai, J. Z. Zhang, H. H. Wang and H. D. Li, *in* Proc. 3rd Int. Conf. on Ion Beam Modification of Materials, Grenoble (edited by B. Biasse, G. Destefanis and J. P. Gaillard) (1982), *in Nucl. Instrum. Methods* **209–210** (1983) 867.
[24] V. Ashworth, R. P. M. Procter and W. A. Grant, The application of ion implantation to aqueous corrosion, *in* 'Treatise on Materials Science and Technology', Vol. 18, Academic Press, New York (1980), Chap. 6.
[25] Y. Okabe, M. Iwaki, K. Takahashi, H. Hayashi, S. Namba and K. Yoshida, *Surf. Sci.* **86** (1979) 257.
[26] Y. Okabe, M. Iwaki, K. Takahashi and K. Yoshida, *Jpn. J. Appl. Phys.* **22** (1983) L165.
[27] K. Takahashi, Y. Okabe and M. Iwaki, *Nucl. Instr. Methods* **182/183** (1981) 1009.
[28] V. Ashworth, W. A. Grant, R. P. M. Procter and T. C. Wellington, *Corr. Sci.* **16** (1976) 393.
[29] H. J. Kim, W. B. Carter, R. F. Hochman and E. I. Meletis, *Mater. Sci. Eng.* **69** (1985) 297.
[30] T. Fujihana, N. Matsuzawa, Y. Okabe and M. Iwaki., Proceedings of the 3rd Symposium on *Surface Layer Modification by Ion Implantation*, Ionics Publishers, Tokyo (1987) p. 45.
[31] A. H. Al-Saffar, V. Ashworth, A. K. O. Bairamov, D. J. Chivers, W. A. Grant and R. P. M. Procter, *Corr. Sci.* **20** (1980) 127.
[32] K. Takahashi, Y. Okabe and M. Iwaki, *J. Chem. Soc. Jpn.* (1983) 784 (in Japanese).
[33] Y. Okabe, K. Takahashi, M. Iwaki and K. Yoshida, *J. Chem. Soc. Jpn.* (1985) 1087.
[34] *Bulg. Pat. 63 360* (1983).
[35] *Bulg. Pat. 29 959* (1982).
[36] W. W. Hu, C. R. Clayton, H. Herman and J. K. Hirvonen, *J. Mater. Sci. & Eng.* **45** (1980) 263.
[37] S. B. Agarwal, PhD dissertation, State University of New York at Stony Brook (1979).
[38] M. Nikolova, G. Raichevski, St. Rashkov and M. Klaua, *Galvanotechnik* **82**(7), (1991) 2321.